Hysteresis effects at the tilted to nontilted transition in octadecanol monolayers as observed with Brewster angle autocorrelation spectroscopy

Cite as: J. Chem. Phys. **106**, 7448 (1997); https://doi.org/10.1063/1.473704
Submitted: 24 October 1996 . Accepted: 24 January 1997 . Published Online: 04 June 1998

C. Lautz, Th. M. Fischer, and J. Kildea

Hysteresis effects at the tilted to nontilted transition in octadecanol monolayers as observed with Brewster angle autocorrelation spectroscopy

C. Lautz and Th. M. Fischer
Fakultät für Physik, Universität Leipzig, Linnéstrasse 5, 04103 Leipzig, Germany

J. Kildea
Alaska Pacific University, 4101 University Drive, Anchorage, Alaska

(Received 24 October 1996; accepted 24 January 1997)

With Brewster angle autocorrelation spectroscopy involving a combination of Brewster angle microscopy and autocorrelation technique we present quantitative measurements of the tilt angle in octadecanol carried out at the triple point of the next nearest neighbor tilted L_2', the nontilted destorted hexagonal LS(Rot I), and the hexagonal LS(Rot II) phases. We show that the transition from the tilted phase to the nontilted phases, which changes from first order (L_2'/LS(Rot I)) to second order (L_2'/LS(Rot II)), is associated with strong hysteresis effects in the L_2' phase, leading to an ambiguity of the tilt angle in the vicinty of the triple point. The behavior gives indications for a hindered first-order phase transition within the L_2' phase. © *1997 American Institute of Physics.* [S0021-9606(97)50817-8]

INTRODUCTION

The phase behavior of Langmuir monolayers has been investigated for many years starting with classical surface pressure isotherm experiments.[1–3] The molecular structure associated with the variety of phase transitions occuring in these films has been revealed using neutron and x-ray diffraction,[4–6] x-ray reflection,[7,8] and optical methods, such as polarized fluorescence[9–11] and Brewster angle microscopy.[12–14] The monolayers usually exhibit crystalline phases at low temperatures, hexatic phases at intermediate temperatures, and liquid and gas phases at high temperatures.[15] The hexatic monolayer phases are associated with a short-range positional order and a quasi-long-range bond orientational order. The difference between the various hexatic phases is described by the tilt order, the tilt azimuth order, and the distortion of the hexagonal packing.[16,17] There are tilted phases at low and nontilted phases at high surface pressure. While the temperature and pressure dependence of the positional bond orientational and tilt order is understood quite well and generally the same for all simple amphiphiles (alcohols, esters and acids), the tilt azimuth order and distortion order parameter show a behavior that is different in long chain alcohols and long chain acids. In heneicosanoic acid for example, there is a transition from an untilted destorted phase LS(Rot I) (low temperature) to an untilted undestorted phase LS(Rot II) (high temperature) which changes to a transition from a distorted phase with the tilt azimuth in direction of the next nearest neighbors L_2' (low temperature) to another distorted phase with the tilt azimuth pointing toward the nearest neighbors L_2 (high temperature) when expanding into the tilted phases. The continuity of the phase transition line suggests that the distortion and the tilt azimuth order are somehow interrelated. However in long chain alcohols the LS(Rot I) to LS(Rot II) transition occurs as well, but the phase transition line does not continue in the tilted phase and there is only a next nearest neighbor distorted hexagonal phase L_2'. Fischer, Teer, and Knobler[18] have carried out optical measurements on acid alcohol mixtures, revealing that the L_2/L_2' transition and the L_2/OV transition both join at concentrations acid:alcohol of 22:78 and are disconnected from the tilted/nontilted transition and LS(Rot I)/LS(Rot II) transition at higher alcohol concentrations. Teer *et al.*[19] have associated the L_2/L_2' transition with the interaction of the hydrated headgroups. Shih *et al.*[20] gave a similar explanation for the L_2/L_2' transition and associated the LS(Rot I)/LS(Rot II) transition with the tail–tail interaction of the molecules. The arguments are convincing because the phase behavior of the alcohols and acids is the same in the untilted phase, while the different headgroups lead to a different phase behavior in the tilted phases. However, the question remains, why does the L_2/L_2' transition join with the LS(Rot I)/LS(Rot II) transition in the acids and what is the interrelation between the distortion and the tilt azimuth order? If there is any relation, how does it effect the behavior of the alcohols in the tilted L_2' phase at pressures slightly below the LS(Rot I)/LS(Rot II) transition?

We tried to address the last question by doing quantitative measurements of the tilt angle behavior in the vicinity of the triple point L_2'/LS(Rot I)/LS(Rot II) using Brewster angle autocorrelation spectroscopy. We found, that the tilt angle in the L_2' phase in the vicinity of the triple point depends on the history and the path taken in the phase diagram. The hysteresis effects may be understood as a hindered first-order phase transition from a less tilted to a more tilted phase. The difference in phase behavior of the alcohols compared with the acids would be that in both samples the destorted nondestorted hexagonal phase transition in the untilted region continues to low pressures in the tilted phase, but the hysteresis in the tilted phase of the alcohol is strong enough that one cannot reach the other phase by just crossing the phase transition line.

 0021-9606/97/106(17)/7448/6/$10.00

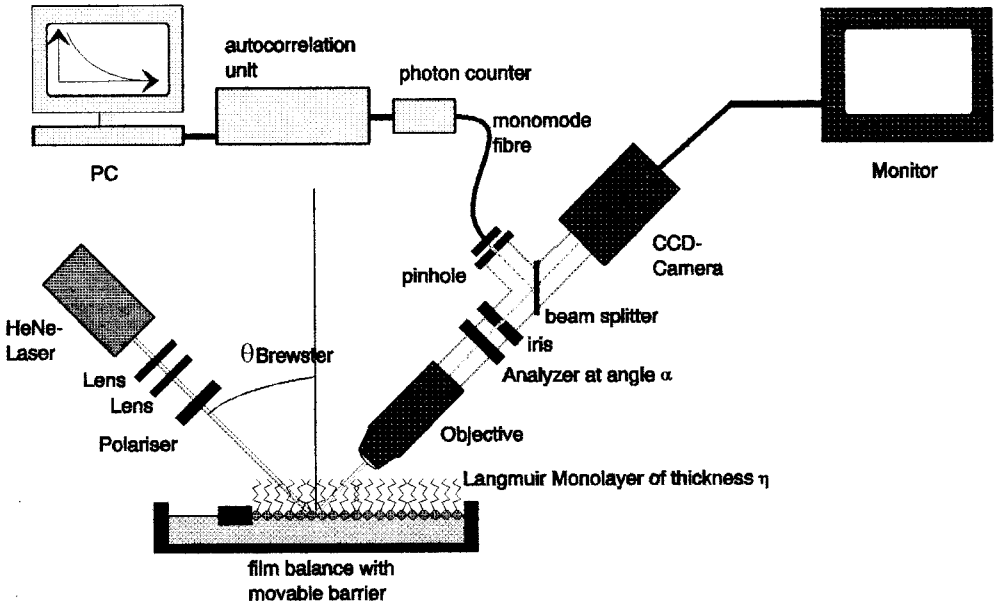

FIG. 1. Schematic diagram of the Brewster angle autocorrelation spectroscope.

EXPERIMENT

The home-built Brewster angle spectroscope allows both to carry out static measurements like investigations of phase transitions of first and second order in Langmuir monolayers and to make dynamic measurements with the autocorrelation unit joined to the Brewster angle microscope by a beam splitter and a single-mode fiber (see Figure 1). With this configuration it is possible to obtain autocorrelation spectra during simultaneous observation of the monolayer on the monitor. An iris in front of the beam splitter and a pinhole (hole diameter: 1 mm) in front of the singlemode fiber allows a precise determination of the region of the monolayer. With the 10× objective the diameter of the spot is smaller than 20 μm. A HeNe laser (Carl Zeiss Jena, HNA 188 S, 60 mW) is focused on the monolayer surface by a telescope arrangement consisting of two lenses ($f_1=10$ mm, $f_2=16$ mm) to increase the intensity at the photon counter. The other components comprising the Brewster angle microscope are a Glan–Thompson polarizer and analyzer (Bernhard Halle Nachfl.) with extinction coefficients of 10^{-8} and 10^{-6}, respectively, a microscope objective (Nikon, MTJ-67-100, 10×, aperture 0.35, working distance 20 mm), and a charge-coupled-device (CCD) camera with a minimum sensitvity of 0.15 lux (SL Microtest GmbH, Jena). The autocorrelation unit consits of a photon counter (ALV/SO-SIPD) and a Multiple Tau Digital Correlator (ALV-5000 fast) plugged on the motherboard of a personal computer allowing one to obtain correlation functions in a time range between 10 ns and a few seconds. For our investigations the correlation functions in a time range between 1 ms and 100 s are shown.

The temperature, the surface pressure, the position, and velocity of the motor driven barrier of the film balance is controlled by a film balance control unit (FiWaS 951, PC-Project).

The home-built film balance consists of a Teflon trough with inner side lengths of 70 mm and 120 mm and a depth of 5 mm. The copper bottom is coated with a 0.3 mm thin Teflon foil. The trough was heated or cooled by two water cooled Peltier elements mounted directly on the back side of the copper sheet. The two Peltier elements cover about 80% of the trough bottom. These geometric dimensions make it possible to obtain measurements with a sufficient thermal stability.

A light flow of the monolayer is induced by a ventilator positioned 30 cm from the trough. The ventilator is blowing away from the trough leading to a diffuse air flow with changing directions. While these experiments were performed no significant changes in temperature and surface pressure could be detected. If the monolayer is exposed to the flow longer than 15 min, deformation of the monolayer into stretched and elongated domains can be seen in the Brewster angle image. For this reason correlation times no longer than 3 min were used. In this time range no differences in domain shape and size was observed compared to the monolayer without flow. We therefore conclude that interactions of flow and texture of the monolayer is negligible. As the domains of different reflectivity flow through the spot of measurement correlation functions with a typical decay rate of several 100 msc are obtained. Clear and reproducible results were achieved with a sample time of 3 min. All autocorrelation measurements were done with simultaneous observation of the monolayer on the TV screen. Identical conditions like domain size and purity of the monolayer could be controlled in this way.

The alcohol used was octadecanol ($C_{18}H_{38}O$) obtained from Sigma Aldrich and claimed to be 99+% pure. Without further purification it was spread from chloroform (p.a.

Merck) onto pure water (Millipore Milli-Q at 18 MΩ) contained in a home-built Teflon trough.

EVALUATION

There have been several approaches to extract information about the tilt angle[21] and the tilt azimuth angle[22] using Brewster angle microscopy. Hosoi *et al.*[21] determined the tilt angle in octadecanoic acid by fitting it to the contrast, i.e., the normalized difference of the brightest and darkest domain of the monolayer. Tsao and co-workers[22] used the symmetry of six star-shaped droplets in methyl eicosanoate to fit the tilt angle and the tilt azimuth angle at the same time. The methods described above all rely on image analysis of Brewster angle microscope pictures.

With Brewster angle autocorrelation spectroscopy we have a more direct measurement of the tilt angle. As different domains of the monolayer flow through the correlation spot the intensity fluctuates because of the different reflectivities. The autocorrelation function

$$g_2=\frac{\langle I(t)I(t+\tau)\rangle}{\langle I(t)\rangle^2} \tag{1}$$

therefore shows a decay as a function of time, which is proportional to the contrast of the different domains. The decay height is given by

$$g_2(\tau=0)-g_2(\tau\rightarrow\infty)=\Delta g_2=\frac{\langle (I-\langle I\rangle)^2\rangle}{\langle I\rangle^2}, \tag{2}$$

where $\langle\rangle$ denotes the time average.

Since all tilt azimuth directions have the same free energy, there is no preference tilt azimuth direction and as time passes all possible tilt azimuth directions occur with the same probability. The time average thus may be replaced by an average over the tilt azimuth directions, i.e.,

$$\Delta g_2=\frac{\overline{(I-\overline{I})^2}}{\overline{I}^2}, \tag{3}$$

with the bar denoting the tilt azimuth average, i.e., $\overline{A}=(1/2\pi)\int A(\varphi)d\varphi$. The dependence of the reflected intensity from the anisotropic monolayer may be solved to first order in the thickness of the monolayer, using the Berreman formalism.[23] The derivation can be found elsewhere.[24] At the Brewster angle it takes the form

$$I_\alpha(\varphi)=(A\ \cos^2\ \varphi+B+C\ \sin\ \varphi+D\ \sin\ \varphi\ \cos\ \varphi)^2, \tag{4}$$

where

$$\begin{aligned}
A&=\frac{\eta}{2\cos\ \Theta_B}\cos\ \alpha\ \sin^2\ \vartheta\ \cos^2\ \Theta_B\\
&\quad\times\delta\chi\ \frac{1+\chi}{1+\chi+\delta\chi\ \cos^2\ \vartheta},\\
B&=\frac{\eta}{2\cos\ \Theta_B}\left(\chi\ \cos\ \alpha\ \cos^2\ \Theta_B\right.\\
&\quad\left.-\cos\ \alpha\ \sin^2\ \Theta_B\ \frac{\chi+\delta\chi\ \cos^2\ \vartheta}{1+\chi+\delta\chi\ \cos^2\ \vartheta}\right),\\
C&=\frac{\eta}{2\cos\ \Theta_B}\cos\ \vartheta\ \frac{2\sin\ \alpha\ \cos^3\ \Theta_B\delta\chi\sin\ \vartheta}{1+\chi+\delta\chi\ \cos^2\ \vartheta},\\
D&=\frac{\eta}{2\cos\ \Theta_B}2\ \sin\ \alpha\ \cos^3\ \Theta_B(1+\chi)\\
&\quad\times\sin\ \vartheta\ \frac{\delta\chi\ \sin\ \vartheta}{1+\chi+\delta\chi\ \cos^2\ \vartheta},
\end{aligned} \tag{5}$$

with η the thickness of the monolayer times 2π over the wavelength, Θ_B the Brewster angle, χ the susceptibility perpendicular to the aliphatic chain, $\chi+\delta\chi$ the susceptibility along the aliphatic chain, ϑ the tilt angle, and α the analyzer angle. Inserting Eq. (4) into Eq. (3) we obtain

$$\Delta g_2=\frac{\frac{17}{128}A^4+\frac{1}{8}C^4+\frac{1}{128}D^4+\frac{1}{2}A^2B^2+\frac{9}{64}A^2D^2+2B^2C^2+\frac{1}{2}B^2D^2+\frac{1}{4}C^2D^2+\frac{1}{2}A^3B+\frac{1}{2}ABC^2+\frac{1}{2}ABD^2}{(\frac{3}{8}A^2+B^2+\frac{1}{2}C^2+\frac{1}{8}D^2+AB)^2}. \tag{6}$$

The plateau height Δg_2 does not depend on the film thickness η. The Brewster angle and the analyzer angle are known from the experiment. The values of the susceptibility along ($\chi+\delta\chi=1.43$) and perpendicular ($\chi=1.25$) to the aliphatic chain are well known for the simple amphiphiles[21] used in this article. We therefore obtain a relationship between the tilt angle ϑ and Δg_2, involving no fit parameter. The relationship of *sqrt*(Δg_2) and ϑ is plotted in Figure 2 for $\Theta_B=53.12°$ and $\alpha=80°$. For these values ϑ is approximately proportional to *sqrt*(Δg_2) for tilt angles in a range from 0° to 13°. In our measurements (compare the autocorrelation function at 3.5 mN/m in Figure 4) the maximal value of Δg_2 is 0.4 corresponding to a tilt angle of 15°. Therefore the relationship $\vartheta\propto\Delta g_2$ holds for all of our measurements.

RESULTS

The phase diagram of octadecanol is shown in Figure 3. It has been first determined by Harkins and Copeland[1] and Shih *et al.*[6] using x-ray diffraction. The phase transition from the tilted L_2' phase to the untilted S and LS(Rot II) phase is of second order, while the transition from the L_2' to the LS(Rot I) is of first order.

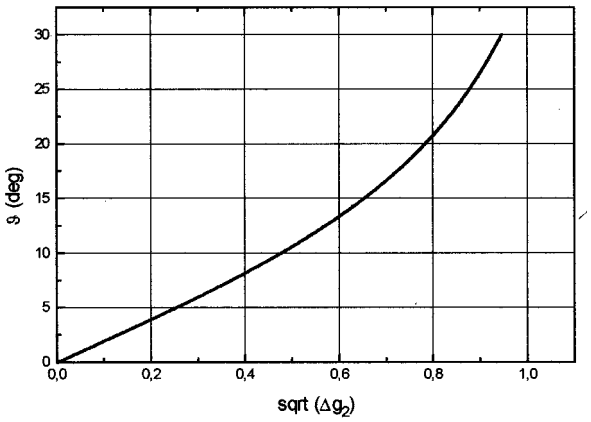

FIG. 2. Relation calculated between $sqrt(\Delta g_2)$ and the tilt angle ϑ.

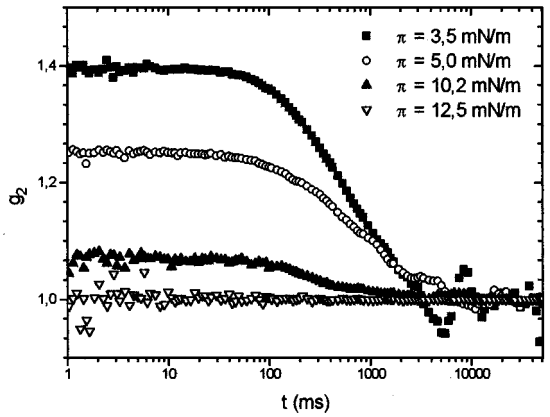

FIG. 4. Autocorrelation functions of octadecanol at different surface pressures (see legend) obtained at $T=20.5$ °C.

The autocorrelation function at $T = 20.5$ °C is plotted in Figure 4 for different surface pressures. As one can see the plateau height decreases continously as the surface pressure increases. For delay times from 100 to 2000 ms the autocorrelation function decreases from the plateau height to 1. This time range corresponds to the distribution of time duration in which the different domains flow through the correlation spot. For times longer than 2000 ms the signal is completely uncorrelated. No differences can be seen between the different surface pressures in this region. The behavior of the square root of the plateau height (the tilt angle) on increasing surface pressure is shown in more detail in figure 5 at $T = 9.0$ °C (L_2'/LS(Rot I) transition) and $T=21.0$ °C (L_2'/LS(Rot II) transition). The difference in order of the tilt/nontilt transition can be clearly seen. At 9.0 °C there is an aprupt change in tilt angle from about 8° at 11.1 mN/m to zero tilt at 11.2 mN/m, while the decrease within the tilted phase from zero pressure to 11.1 mN/m is only about 40% (from 15° to 8°). At $T=21.0$ °C the tilt angle changes continously from 15° at zero pressure to 3° at 12.4 mN/m and zero at 12.5 mN/m. As one can see from these data the tilt angle slightly below the tilt/nontilt pressure has quite different values at $T=9.0$ °C and $T=21.0$ °C. How does it change from low values at high temperature to high values at low temperature, when approaching and crossing the triple point (L_2'/LS(Rot I)/LS(Rot II)), where the order of the transition changes? Figure 6 shows the tilt angle behavior in the vicinity of the triple point. In contrast to the measurements in Figure 5 the values of $sqrt(\Delta g_2)$ are obtained by leaving the LS(Rot I) and LS(Rot II) phase respectively and entering the L_2' phase by isothermal expansion. In case of the second-order phase transition between the LS(Rot II) and the L_2' phase, we waited approximately 10 min before starting the autocorrelation measurements. This ensured that the domains could heal and then were larger than the spot on the monolayer detected by the photon counter. The data in Figure 6

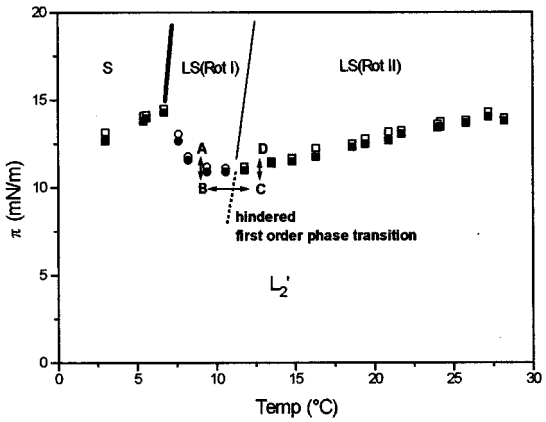

FIG. 3. Phase diagram of ocotadecanol obtained with Brewster angle microscopy (dotted line) and x-ray diffraction (Ref. 6) (solid lines). The open symbols represent results obtained with increasing, the solid symbols with decreasing surface pressure. First-order phase transitions are shown by circles, second-order phase transitions by squares. The thick line represents a phase transition of first order, the thin line a phase transition of second order. The points A,B,C,D represent distinguished points in the phase diagram.

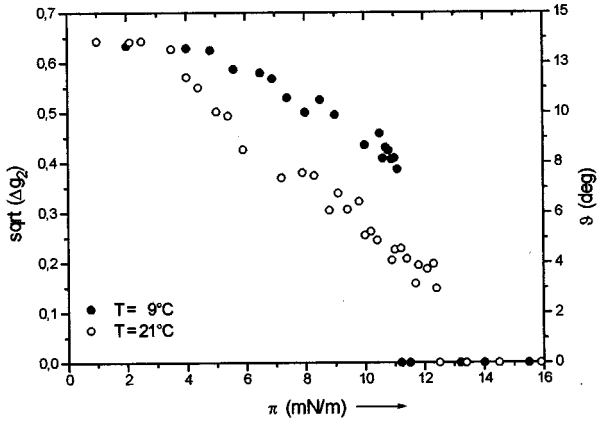

FIG. 5. Relation between $sqrt(\Delta g_2)$, tilt angle ϑ, and surface pressure π, obtained from autocorrelation measurements of octadecanol at 9 and 21 °C.

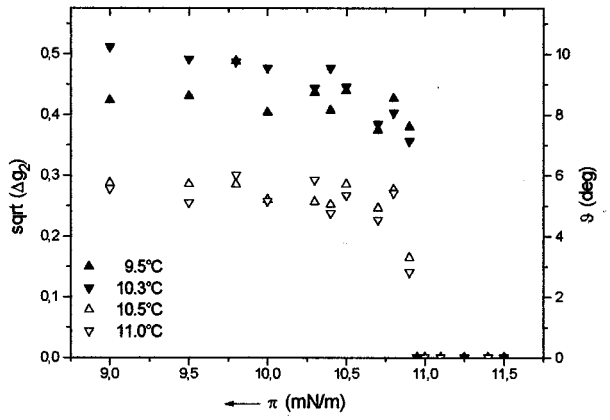

FIG. 6. Relation between $sqrt(\Delta g_2)$, tilt angle ϑ, and surface pressure π, obtained from autocorrelation measurements of octadecanol near the triple point at different temperatures (see legend).

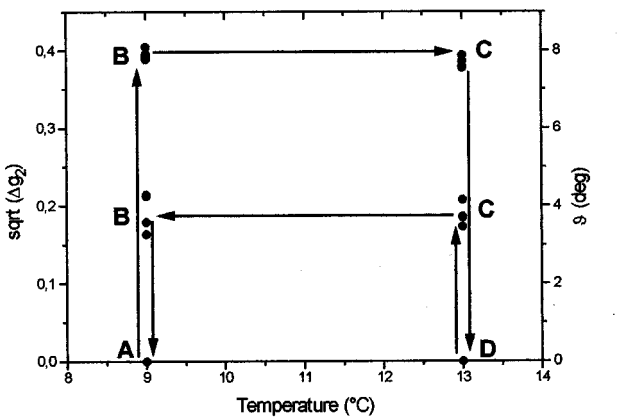

FIG. 7. $sqrt(\Delta g_2)$ and tilt angle ϑ as a function of temperature depending on the different path taken between the four points A,B,C,D in the phase diagram shown in Figure 3.

reveal a surprising effect. The tilt angle obtained below the transition nontilted/tilted stays at approximately 7.5° even at 10.3 °C slightly below the temperature of the triple point, and stays low at 10.5 °C slightly above the triple point temperature. Of course the differences in the tilt angle can be also seen qualitatively in the Brewster angle microscope images. There is a jump in tilt angle from 8° to 3° within a temperature interval of 0.2 °C in the L_2' phase, indicating that there is a first-order transition from one tilted L_2' phase to an L_2' phase of different tilt angle. As in acids the transition line LS(Rot I)/LS(Rot II) would continue into the tilted phase separating now two tilted phases with different tilt angle. Why did nobody see this transition so far? On isobaric heating or cooling across 10.4 °C one would expect to see a change in contrast of the Brewster angle microscopy images. We measured the tilt angle near the triple point, following the path shown in the phase diagram in Figure 3. We started in the untilted LS(Rot I) phase in point A ($T=9$ °C, $\pi=13$ mN/m) following along an isotherm to point B in the high tilted L_2' phase, heating to point C along an isobar and then isothermal compressing to the untilted LS(Rot II) phase. The same experiment was performed in the opposite direction. The result of this experiment is shown in Figure 7. The tilt angle obtained in point B when expanding from the point A is consistent with those presented in Figure 6. If we now heat up to point C the tilt angle does not change and stays at approximately 7.5°. On compressing into the LS(Rot II) phase the tilt angle vanishes at point D. Expanding back to C now gives a tilt angle of 3° in accordance with the values obtained in Figure 6. Cooling to B does not change this tilt angle. On compression to A the tilt again vanishes. As one can see from Figure 7 no first-order phase transition happened, neither on isobaric heating nor on isobaric cooling. The original tilted phase obtained on isothermal expansion is maintained instead. The experiment was repeated three times. As one can see in Figure 7 the hysteresis is completely reproducible. The domain structure and the tilt angle in any points of the L_2' phase near the triple point depend only on the path in the phase diagram taken to reach these points (memory effect). This memory effect is no longer visible far away from the triple point, i.e., at lower surface pressure, e.g., 5 mN/m.

The clear differences in tilt angle behavior in the L_2' phase in a small temperature region between 10.3 and 10.5 °C indicate a first-order phase transition. However, this transition cannot neither be induced on isobaric heating nor cooling due to strong supercooling and superheating effects. This is the reason that this transition has not been observed so far.

CONCLUSION

With Brewster angle autocorrelation spectroscopy we introduced a useful tool for measurements of the tilt angle in Langmuir monolayers. The behavior of the tilt angle in octadecanol has been investigated. Clear differences in the autocorrelation measurements between first- and second-order phase transitions allowed us to investigate the tilt angle behavior on the triple point L_2'/LS(Rot I)/LS(Rot II). We found strong changes of the tilt angle in the L_2' phase and memory effects indicating a hindered first-order phase transition.

ACKNOWLEDGMENT

This work was supported by the Sonderforschungsbereich SFB 294.

[1] W. D. Harkins and L. E. Copeland, J. Chem Phys. **10**, 272 (1942).
[2] M. Lundquist, Chem. Scr. **1**, 197 (1971).
[3] S. Ställberg-Stenhagen and E. Stenhagen, Nature **146**, 240 (1945).
[4] R. M. Kenn, C. Böhm, A. M. Bibo, I. R. Peterson, and H. Möhwald, J. Phys. Chem. **95**, 2092 (1991).
[5] B. Lin, M. C. Shih, T. M. Bohanon, G. E. Ice, and P. Dutta, Phys. Rev. Lett. **65**, 191 (1990).
[6] M. C. Shih, T. M. Bohanon, J. M. Mikrut, P. Zschack, and P. Dutta, Phys. Rev. A **45**, 5734 (1992).
[7] M. L. Schlossman and P. S. Pershan, in *Light Scattering by Liquid Surfaces*, edited by D. Langevin (Dekker, New York, 1992), p. 365.
[8] J. Als-Nielsen and H. Möhwald, in *Handbook on Synchroton Radiation*,

edited by S. Ebashi, E. Rubenstein, and M. Koch (North-Holland, Amsterdam, 1989), p. 4.1.
[9] M. Lösche, E. Sackmann, and H. Möhwald, Ber. Bunsenges. Phys. Chem. **87**, 848 (1983).
[10] H. M. McConnel, L. K. Tann, and R. M. Weiss, Proc. Natl. Acad. Sci. (USA) **81**, 3249 (1984); R. M. Weiss and H. M. McConnell, Nature **310**, 47 (1984); H. E. Gaub, V. T. Moy, and H. M. McConnell, J. Phys. Chem. **90**, 1721 (1986).
[11] B. Moore, Ch. M. Knobler, D. Brossetan, and F. Rondelez, J. Chem. Soc. Faraday Trans. 2 **82**, 1753 (1986); F. Rondelez and K. A. Suresh, in Physics of Anphiphilic Layers, edited by J. Meunier, D. Langevin, and N. Boccara (Springer, Berlin, 1987), p. 20.
[12] S. Hénon and J. Meunier, Rev. Sci. Instrum. **62**, 936 (1991).
[13] D. Hönig and D. Möbius, J. Phys. Chem. **95**, 4590 (1991).
[14] S. Hénon and J. Meunier, J. Chem. Phys. **98**, 9148 (1993).
[15] C. M. Knobler and R. C. Desai, Ann. Rev. Phys. Chem. **43**, 207 (1992).
[16] G. W. Gray and J. W. Goodby, *Smectic Liquid Crystals: Textures and Structures* (World Scientific, Singapore 1988).
[17] J. d. Brock, R. J. Birgenau, J. D. Litster, and A. Aharony, Phys. Today **42**, 52 (1989).
[18] B. Fischer, E. Teer, and C. M. Knobler, J. Chem. Phys. **103**, 2365 (1995).
[19] E. Teer, C. M. Knobler, C. Lautz, S. Wurlitzer, J. Kildea, and T. M. Fischer, J. Chem. Phys. **106**, 1913 (1997).
[20] M. C. Shih, M. K. Durbin, A. Malik, and P. Dutta, J. Chem. Phys. **101**, 9132 (1994).
[21] K. Hosoi, T. Ishikawa, A. Tomioka, and K. Miyano, Jpn. J. Appl. Phys. **32**, 135 (1993).
[22] M.-W. Tsao, Th. M. Fischer, and Ch. M. Knobler, Langmuir **11**, 3184 (1995).
[23] D. Berreman, J. Opt. Soc. Am. **62**, 502 (1972).
[24] Y. Tabe and H. Yokoyama, Langmuir **11**, 699 (1995).